Control of offset field and pinning stability in perpendicular magnetic tunnelling junctions with synthetic antiferromagnetic coupling multilayer

Guchang Han, Michael Tran, Cheow Hin Sim, Jacob Chenchen Wang, Kwaku Eason, Sze Ter Lim, and Aihong Huang

Citation: Journal of Applied Physics **117**, 17B515 (2015); doi: 10.1063/1.4913942
View online: http://dx.doi.org/10.1063/1.4913942
View Table of Contents: http://scitation.aip.org/content/aip/journal/jap/117/17?ver=pdfcov
Published by the AIP Publishing

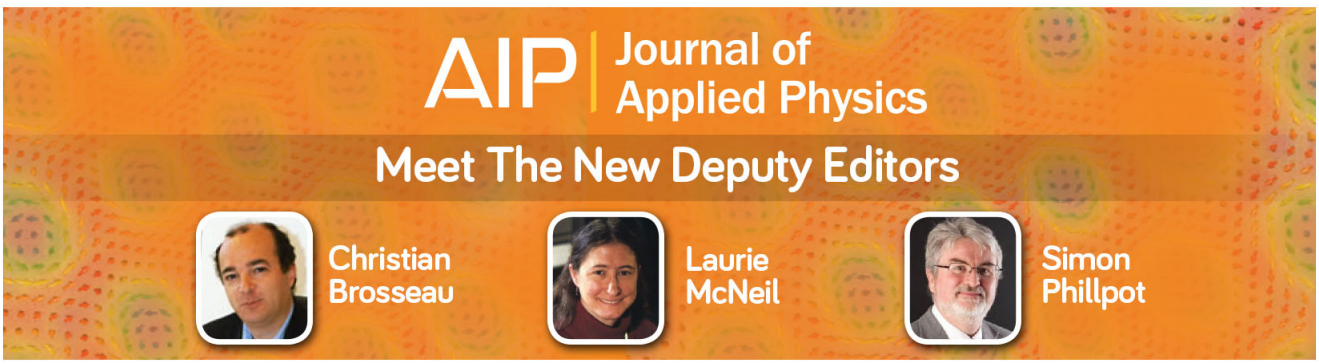

JOURNAL OF APPLIED PHYSICS **117**, 17B515 (2015)

Control of offset field and pinning stability in perpendicular magnetic tunnelling junctions with synthetic antiferromagnetic coupling multilayer

Guchang Han,[a] Michael Tran, Cheow Hin Sim, Jacob Chenchen Wang, Kwaku Eason, Sze Ter Lim, and Aihong Huang
*Data Storage Institute, A*STAR (Agency for Science Technology and Research), 5 Engineering Drive 1, DSI Building, Singapore 117608, Singapore*

(Presented 5 November 2014; received 18 September 2014; accepted 30 October 2014; published online 9 March 2015)

In a magnetic tunnelling junction (MTJ) with perpendicular magnetic anisotropy (PMA), offset field (H_o) of the free layer is usually controlled by using a synthetic antiferromagnetic (SAF) coupling structure, which is composed of an antiferromagnetic coupling (AFC) layer sandwiched by two ferromagnetic (FM) layers. However, H_o increases significantly as the size of MTJ devices shrinks to accommodate high density. In addition, magnetostatic field in PMA SAF structure tends to destabilize the antiferromagnetic (AFM) alignment of the SAF layers, in contrast to the in-plane anisotropy SAF, where the closed flux forms stable AFM magnetic configuration. Here, we present a double SAF structure to control H_o, while maintaining high magnetic stability of the reference layer (RL). The double SAF consists of FM1/AFC/FM2/AFC/FM3 multilayer. An AFM layer like PtMn is added to further stabilize the magnetic configuration of the double SAF. As the magnetization of other FM layers (FM1 and FM2) is aligned oppositely, the magnetostatic field acting on the RL (FM3) layer is significantly reduced due to cancellation effect from its adjacent layers. Both simulation and experimental results demonstrate that the double SAF layers provide high stability for the RL in addition to the reduction of H_o. Our results on MTJ devices show that the AFM pinned double SAF has the highest RL stability. The RL switch rate decreases as the thickness of the CoFe inserted layer between AFM and the pinned layer (Co/Pt multilayer) increases due to improved exchange coupling. © *2015 AIP Publishing LLC*. [http://dx.doi.org/10.1063/1.4913942]

I. INTRODUCTION

Magnetic tunnelling junctions (MTJs) with perpendicular magnetic anisotropy (PMA) are the most promising devices for high density magnetic random access memory (MRAM).[1–8] To realize the practical applications of MRAM, MTJ elements must meet a set of performance requirements such as high thermal stability for data retention, low switching current, and narrow distribution, as well as scalability. A MTJ device is composed of several material layers, typically including a reference layer (RL), a barrier layer, and a storage (free) layer (FL). RL has a fixed magnetization direction, while the magnetization direction of FL can be switched to define data state of "0" or "1." Therefore, it is essential that the switching field of RL should be as high as possible to avoid magnetization switching against disturbance. On the other hand, the FL magnetization direction should be changed easily during programing, while kept stably for data retention. The thermal stability of the FL is critical for data storage application as it requires long data retention. It has been reported that the stray field from the RL may influence the thermal stability of the FL.[9] The stray field induces the shift of magnetoresistance (R-H) curve from zero field, resulting in an offset field (H_o) for the FL operation. In the extreme case, when the H_o exceeds the coercivity field of the FL, the bistable states will no longer exist in the absence of a magnetic field, thus losing data. Therefore, H_o must be properly controlled. H_o is usually suppressed by using a synthetic antiferromagnetic (SAF) coupling reference structure.[10] However, H_o becomes increasingly difficult to control as it will escalate when the size of MTJ devices is scaled down to accommodate high density.[11] In addition, magnetostatic field in PMA SAF structure tends to destabilize the antiferromagnetic (AFM) alignment of SAF layers, in contrast to the in-plane anisotropy SAF layers, where the closed flux forms stable AFM configuration. Therefore, it is imperative for a stack structure to effectively control H_o, while keeping the magnetization stability of the RL in perpendicular MTJs. It has been shown that H_o can be reduced by extending RL edge of a PMA-MTJ such that the pinned RL is wider than the free layer.[12] This stepped structure requires an etching process that stops at the tunnel barrier and thus increases the process complexity. In addition, H_o would depend on etching process significantly. Another method is to use toppings with a stack structure similar to a dual spin valve to compensate the stray field in MTJs with in-plane anisotropy.[13] Very recently, a counter bias layer is proposed to suppress the offset field in a top-pinned PMA MTJ.[14] However, the stray field from this bias layer may also induce the instability of the RL in spite of being smaller than that from the pinned layer in a SAF structure. Here, we present a double SAF structure to control H_o, while maintaining high magnetic stability of the RL. It is found that the RL is much more stable when the double SAF multilayer is effectively pinned by an AFM layer.

[a]Author to whom correspondence should be addressed. Electronic mail: han_guchang@dsi.a-star.edu.sg.

II. WORKING PRINCIPLE OF DOUBLE SAF MULTILAYER

Fig. 1(a) shows a typical MTJ stack structure with bottom pinned double SAF reference multilayer. The double SAF consists of FM1/AFC/FM2/AFC/FM3 multilayer, where FM is a ferromagnetic layer and AFC is an AFM coupling layer. An AFM layer like PtMn is added to further stabilize the magnetic configuration of the double SAF multilayer. In order to make the double SAF multilayer more stably pinned by AFM layer, it is desirable to have a balanced magnetic structure, which means the net magnetic moment from the double SAF multilayer is close to zero, i.e., $(M_rt)_2 = (M_rt)_1 + (M_rt)_3$ (refer to Fig. 1(a). H_o can be controlled by varying thickness combination of three magnetic layers, while keeping the net magnetic moment of SAF multilayer nearly zero. On the other hand, for a single SAF pinning structure, where FM1 is removed, a magnetically balanced structure would have $(M_rt)_2 = (M_rt)_3$. However, the stray field in this balanced SAF structure would increase significantly as MTJ size decreases. As an example, Fig. 1(b) shows simulated stray field averaged over the FL for a single SAF with 2 nm-thick FM2 and FM3 layers as a function of MTJ size. The stray field can be as high as several hundreds of Oe for a MTJ of 20×20 nm. In order to reduce the stray field generated from SAF multilayer, $(M_rt)_2$ has to be larger than $(M_rt)_3$ so that its spatial loss of the stray field at the FL can be compensated by the larger moment. In this unbalanced magnetic structure, the pinning stability is purely maintained by PMA of each FM layer. Once they are aligned parallel to each other, which may be energetically favored due to magnetostatic interaction, an initialization process, e.g., applying a sufficiently high in-plane field to MTJs, has to be conducted to get an antiparallel magnetic configuration. However, as PMA is largely determined by the repeat number in commonly used Co/Pt or Co/Pd multilayers,[15,16] high PMA will generally require thicker FM2 and FM3 layers. Thick FM3 and FM2 layers would in turn induce significant spatial loss of the stray field, in particular, from the FM2 layer, which is separated from the FL by FM3 and AFC layers. Therefore, the magnetic moment of FM2 layer should be increasingly surplus that of FM3 layers to compensate the spatial loss of the stray field. However, large $(M_rt)_2$ would generate a large field at the FM3 (RL) and destabilize the RL. In addition, it would be difficult to pin this unbalanced magnetic structure using an AFM layer as the exchange coupling field is inversely proportional to the net moment of SAF multilayers. Therefore, the pinning through AFC layer would not be sufficient to maintain high stability of the RL. On the other hand, in the double SAF structure, the stray field at the RL from the FM2 layer is compensated by FM1 layer. In addition, as the magnetization of the RL can be fixed through Ru AFC layer due to balanced magnetic configuration which is pinned by the AFM layer, the stability of the RL can be further enhanced. As a result, an ultrathin RL could be used to maintain its magnetic stability.

The inset of Fig. 1(b) shows a typical example of the offset field in a 20 nm × 20 nm MTJ device for three thickness combinations of 2-6-4, 2-7-5, and 2-8-6, where the numbers are the thickness of FM3-FM2-FM1 in nanometer, respectively. The offset field is obtained from simulated R-H curves and defined as the field at the center of R-H loop shifting from zero field. Note that H_o can be effectively reduced to nearly zero with a proper thickness combination, while keeping the overall magnetic moment at about zero. As the magnetization of the adjacent FM layers (FM1 and FM2) is aligned oppositely, the magnetostatic field acting on the RL is significantly reduced due to cancellation effect. Therefore, the RL is much more stable than in the single SAF structure, whereby the magnetostatic field from the pinned layer is much higher. Figs. 2(a) and 2(b), respectively, show the stray field profile at the free layer along the z direction (perpendicular to the plane) and the x-direction (in the plane) from double SAF (circle) and single SAF (square) based on micromagnetics simulations. In this simulation, both ferromagnetic layers are 2 nm thick in single SAF multilayer, while the double SAF has a thickness combination of 2-7-5. In addition to the significant reduction in the stray field in the double SAF, the edge in-plane component of the stray field is reduced significantly, which would make the edge domain more stable and thus improve the stability of the FL.

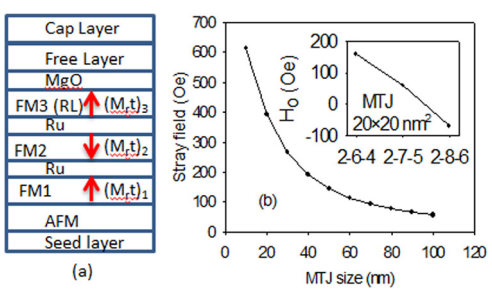

FIG. 1. (a) Schematic layer structure of the proposed double SAF MTJ; (b) averaged stray field at the FL as a function of MTJ size for a single SAF with 2 nm-thick ferromagnetic layers, where the inset shows simulated offset field of 20×20 nm^2 double SAF MTJ with different thickness combination of the ferromagnetic layers.

III. EXPERIMENTS

MTJ stacks with single SAF, double SAF, and AFM pinned double SAF were deposited on Si wafers with 1 μm thermally oxidized SiO_2 using the Singulus Timaris sputtering system. Their stack structures are bottom electrode/Ta 5/Pt 5/[Co 0.5/Pt 0.2]15/Co 0.3/Ru 1.0/[Co 0.5/Pt 0.2]2/Co40Fe40B20 0.6/Ta 0.3/Co40Fe40B20 1.0/MgO 1.1/Co40Fe40B20 1.5/Ta 2/top electrode for wafer A, bottom electrode/Ta 5/Pt 5/PtMn t_{PtMn}/[Co 0.5/Pt 0.2]10/Co 0.3/Ru 1.0/[Co 0.5/Pt 0.2]15/Co 0.3/Ru 1.0/[Co 0.5/Pt 0.2]2/Co40Fe40B20 0.6/Ta 0.3/Co40Fe40B20 1.0/MgO 1.1/Co40Fe40B20 1.5/Ta 2/top electrode for wafer B, and bottom electrode/Ta 5/Pt 5/PtMn 16/CoFe t_{CoFe}/[Co 0.5/

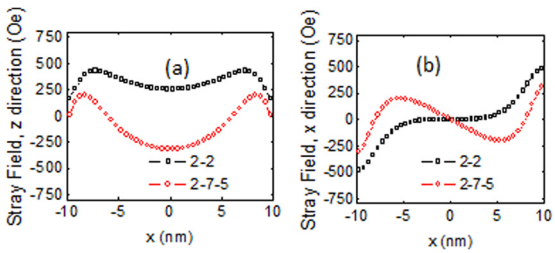

FIG. 2. Stray field profile of 20 nm MTJs with the single SAF (square) and the double SAF (circle) along out of (a) and in (b) the plane directions.

Pt 0.2]10/Co 0.3/Ru 1.0/[Co 0.5/Pt 0.2]15/Co 0.3/Ru 1.0/[Co 0.5/Pt 0.2]2/Co40Fe40B20 0.6/Ta 0.3/Co40Fe40B20 1.0/MgO 1.1/Co40Fe40B20 1.5/Ta 2/top electrode for wafer C, where the number in each layer indicates its thickness in nanometer. A 0.3 nm-thick Ta is inserted to the CoFeB reference layer to tune its magnetic anisotropy and enhance tunnel magnetoresistance (TMR) ratio by improving the crystalline structure of the CoFeB layer near the MgO barrier during the annealing. A single SAF pinning structure is used for wafer A with much thicker FM2 layer (referring to Fig. 1(a), Ru, FM1, and AFM are removed in wafer A). In order to examine PMA exchange coupling effect between AFM and FM1 layers on the stability of the RL, the thickness of the AFM layer, t_{PtMn}, and the insertion layer between AFM and FM1 layers, t_{CoFe} is varied to modulate the PMA exchange coupling in wafers B and C. t_{PtMn} and t_{CoFe} range from 12 nm to 22 nm and 0.5 nm to 1.5 nm, respectively. It should be pointed out that in the above wafer stack structures, in order to demonstrate the advantages of the double SAF over the single SAF, we deliberately used a low-PMA RL so that its magnetic stability can be examined in our maximum measuring field range. Using an optimized multilayer with high PMA, the RL magnetization can be well maintained above a field of 3 kOe even using single SAF structure. To develop an exchange coupling between PtMn and (Co/Pt) multilayer, wafer B and C were annealed at 300 °C for 1 h in a magnetic field of 1 T applied perpendicular to the film plane. The MTJ stacks were fabricated to a circular shape with a nominal diameter of 65 nm using standard photolithography process. The measurements were conducted in a testing station by applying perpendicular magnetic field at a DC bias voltage of 50 mV. Magnetic properties and switching fields of the magnetic layers were extracted from magnetoresistance (R-H) loops. About 250 MTJ devices were measured on each wafer to provide a statistic analysis of overall MTJ performances.

IV. RESULTS AND DISCUSSION

Figs. 3(a), 3(c), and 3(d) show typical R-H curves for three types of samples A, B, and C, respectively. The switching process is illustrated by arrows in Figs. 3(a), 3(b), and 3(c), where the solid arrows indicate switching when field sweeps from 3 kOe to −3 kOe, while the dashed arrows show the opposite sweeping. The bold arrows show the magnetization directions of each FM layer at various field regions. The open bold arrows (red) show the switching layer when the field sweeps from 3 kOe to −3 kOe (e.g., in Fig. 3(a) the FL switches first at a small negative field and then the RL switches at a larger negative field of about −1200 Oe). It is found that for wafers A and B, most of MTJs show RL switching in addition to FL switching within a field range of ±3 kOe, while most MTJs for wafer C do not show RL switching. In addition, H_o decreases from wafers A to B and then to C. It should be pointed out that with PtMn pinning layer, all MTJs in wafers B and C show similar switching order, i.e., FL switches before RL when the field is reduced from 3 kOe to −3 kOe. On the other hand, for MTJs on wafer A, the switching order is randomized. Two types of switching order can be clearly observed as shown in Figs. 3(a) and 3(b). The switching order is determined by the magnetization direction of the FM2 layer, which has a strong PMA and keeps its magnetization fixed in the whole applied field region.

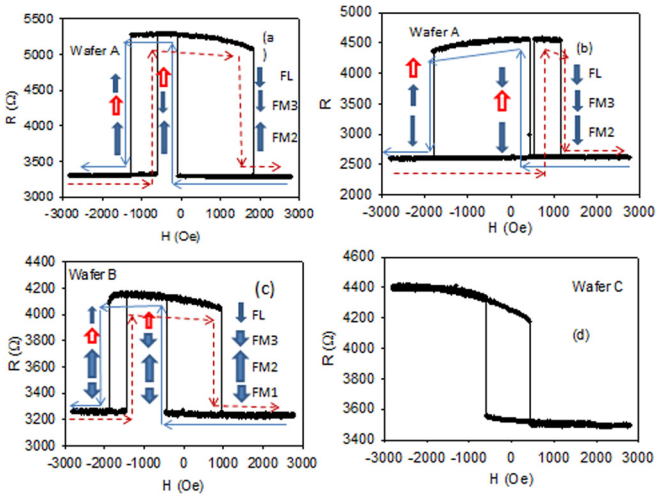

FIG. 3. Typical M-H curves of MTJ devices from wafers A, B, and C. The bold arrows represent the magnetization direction of each layer. The open arrows show the switching layer when the field is ramped down from positive 3 kOe. The switching process is indicated by solid and dotted arrows.

Figs. 3(a) and 3(b) show the magnetization of FM2 layer is aligned anitiparallel and parallel to the positive field direction, respectively. Owing to strong AFM coupling between FM2 and FM3 through Ru, for FM2 parallel to the positive field direction, the RL switches before the FL when the field decreases from 3 kOe to −3 kOe, as shown in Fig. 3(b). The difference in the switching order for MTJs on wafer A can be understood as no setting field is applied for wafer A, while the magnetization of the pinning layer (FM1) on wafers B and C is fixed during annealing. Comparing Figs. 3(a) and 3(c), one can see that the offset field of the FL is much reduced in wafer B. The suppression in H_o is the results from the double SAF as the stray fields at the FL generated from each FM layer are cancelled each other. On the other hand, although the RL switching is still observed, the offset field of RL switching for MTJs from wafer B is much increased from less than 1 kOe for wafer A to near 2 kOe for wafer B as shown in Figs. 3(a) and 3(c).

It is noted that the TMR ratio is lower for wafers B and C than wafer A, which could result from the roughness increase accumulated by PtMn and additional Co/Pt multilayers.

The saturation magnetization (Ms) used for stack design is 1250 emu/cc and 800 emu/cc for CoFeB and (Co0.5/Pt0.2) multilayer, respectively. From the offset field of the free layer observed in Figs. 3(a), 3(b), and 3(c), it appears that either Ms of CoFeB is over-estimated (i.e., actual Ms could be less than 1250 emu/cc) or (Co0.5/Pt0.2) has a higher Ms. As a result, H_o is actually dominated by FM2 layer, resulting in positive H_o values as indicated in Figs. 3(a), 3(c), and 3(d).

However, it is also noted that although an AFM layer has been added to wafer B, the majority of MTJs in this wafer shows RL switching within the field of ±3 kOe, in contrast to those in wafer C. The enhancement in the RL stability for MTJs from wafer C implies that the AFM layer does provide some pinning effect to the SAF multilayers. The survey measurements for MTJs with various t_{PtMn} on wafer B show that the RL switching field is almost independent of t_{PtMn}. Therefore, the RL

instability is not related to the AFM stability due to its thickness variation, but the weak exchange coupling between the AFM and the pinned (FM1) layer. As there is only an ultrathin Co layer of 0.5 nm between the AFM layer (PtMn) and the FM1, the exchange coupling is too weak to provide an effective pinning of the magnetization of FM1 layer, resulting in the magnetization instability of the whole SAF multilayers through AFC coupling. As a result, even for MTJs with thick PtMn layer, the RL switching takes place. On the other hand, for most MTJs on wafer C, the RL is stable within the field of ±3 kOe as shown in Fig. 3(d), due to improved exchange coupling between the AFM and FM1 layers as an additional CoFe layer is inserted between the AFM and FM1 layers. The RL switching observed in a small number of MTJs even on wafer C is due to weak exchange coupling as the inserted CoFe layer is too thin.

Fig. 4 shows a summary result of the offset field for the switching of the RL (H_{ORL}) from about 250 MTJs in each wafer. To get correct switching data for the RL, wafer A was initialized with a magnetic field of 3 T applied perpendicular to the plane so that the magnetization reversal of the RL for all MTJs takes place in the negative field region as shown in Fig. 3(a). To make H_{ORL} comparable with wafers B and C, the initialization field is applied in an opposite direction of the annealing field. One can see that the distribution of H_{ORL} is narrower for wafer A, while the wafer C shows the largest H_{ORL} distribution. Accordingly, the amount of MTJs showing the RL switching is also decreasing from wafers A to B, then to C, indicating the improvement of RL stability. The largest distribution in wafer C is from the thickness wedge of the insertion layer, t_{CoFe}, to enhance the exchange coupling between the AFM layer and FM1 layer. The H_{ORL} distribution in wafer A is purely determined by the process fluctuations. Significant increase in H_{ORL} values is clearly observed for MTJs in wafers B and C, verifying the cancellation effect of the stray field in the double SAF layers on the RL stability. The slight H_{ORL} increase in wafer C compared to wafer B is due to improved pinning effect from the AFM layer. It is worth noticing that the introduction of the insertion CoFe layer between the AFM and FM1 layers would actually decrease H_{ORL} as the stray field at the RL from the FM2, which contributes to H_{ORL} dominantly, would be further compensated by the FM1 layer due to the CoFe insertion.

In order to further confirm the pinning effect on the RL stability, Fig. 5 shows that the switching probability of the RL as a function of t_{CoFe}. The switching rate is defined as

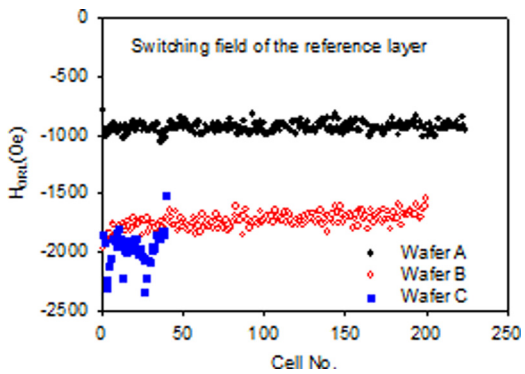

FIG. 4. Offset field for the RL switching for MTJs from wafers A, B, and C.

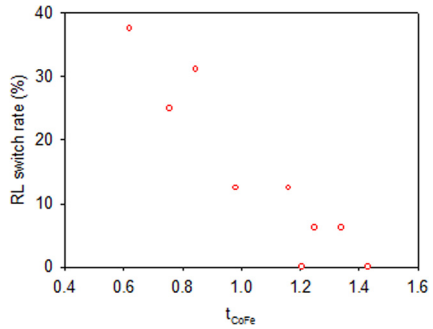

FIG. 5. RL switch rate for MTJs from wafer C as a function of the insertion layer thickness t_{CoFe}.

ratio of the number of MTJs showing the RL switching over the total measured MTJ numbers (10–30) at each t_{CoFe}. In spite of data scattering, which could be induced from the small number of measured MTJs at each t_{CoFe}, it is obvious that the RL switching rate decreases as t_{CoFe} increases. At $t_{CoFe.} > 1.2$ nm, the switching rate is below 5%, which may be induced by the process fluctuations. This result suggests that the strong exchange coupling could be achieved only with thick CoFe insertion layer, and the strong exchange coupling is required to improve the RL stability in the double SAF multilayers. It is noted that even in wafer C, there is a net magnetic moment in the double SAF structure, which would also reduce the stability of the RL.

In conclusion, a double SAF structure is proposed to suppress the offset field, while keep high stability of the reference layer. Experimental results show that the RL switching field can be significantly increased using the double SAF with strong AFM pinning.

[1]J. C. Slonczewski, U.S. patent 5,695,864 (Dec. 9, 1997).
[2]J. Z. Sun, Phys. Rev. B **62**, 570 (2000).
[3]S. Mangin, D. Ravelosona, J. A. Katine, M. J. Carey, B. D. Terris, and E. E. Fullerton, Nat. Mater. **5**, 210 (2006).
[4]H. Meng and J.-P. Wang, Appl. Phys. Lett. **88**, 172506 (2006).
[5]M. Nakayama, T. Kai, N. Shimomura, M. Amano, E. Kitagawa, T. Nagase, M. Yoshikawa, T. Kishi, S. Ikegawa, and H. Yoda, J. Appl. Phys. **103**, 07A710 (2008).
[6]S. Mangin, Y. Henry, D. Ravelosona, J. A. Katine, and E. E. Fullerton, Appl. Phys. Lett. **94**, 012502 (2009).
[7]L. Liu, T. Moriyama, D. C. Ralph, and R. A. Buhrman, Appl. Phys. Lett. **94**, 122508 (2009).
[8]S. Ikeda, K. Miura, H. Yamamoto, K. Mizunuma, H. D. Gan, M. Endo, S. Kanai, J. Hayakawa, F. Matsukura, and H. Ohno, Nat. Mater. **9**, 721 (2010).
[9]H. Sato, M. Yamanouchi, K. Miura, S. Ikeda, H. D. Gan, K. Mizunuma, R. Koizumi, F. Matsukura, and H. Ohno, Appl. Phys. Lett. **99**, 042501 (2011).
[10]D. C. Worledge, G. Hu, D. W. Abraham, J. Z. Sun, P. L. Trouilloud *et al.*, "Spin torque switching of perpendicular Ta/CoFeB/MgO-based magnetic tunnel junctions," Appl. Phys. Lett. **98**, 022501 (2011).
[11]W. S. Zhao, E. Belhaire, C. Chappert, and P. Mazoyer, ACM Trans. Embedded Comput. Syst. **9**(2), 14 (2009).
[12]K. Miura, S. Ikeda, M. Yamanouchi *et al.*, in *VLSI Technology Digest* (IEEE, 2011), p. 214.
[13]K.-M. H. Lenssen, C. Giebeler, and A. E. T. Kuiper, IEEE Trans. Magn. **37**, 1739 (2001).
[14]Y. Iba, C. Yoshida, A. Hatada *et al.*, in *2013 Symposium on VLSI Technology Digest* (IEEE, 2013), p. T136.
[15]S. J. Greaves, P. J. Grundy, and R. J. Pollard, J. Magn. Magn. Mater. **121**, 532 (1993).
[16]A. S. H. Rozatian, C. H. Marrows, T. P. A. Hase, and B. K. Tanner, J. Phys.: Condens. Matter **17**, 3759 (2005).